Wave Breaking Dissipation in the Wave-Driven Ocean Circulation

JUAN M. RESTREPO

Department of Mathematics, and Department of Physics, The University of Arizona, Tucson, Arizona

(Manuscript received 17 April 2006, in final form 13 November 2006)

ABSTRACT

If wave breaking modifies the Lagrangian fluid paths by inducing an uncertainty in the orbit itself and this uncertainty on wave motion time scales is observable as additive noise, it is shown that within the context of a wave–current interaction model for basin- and shelf-scale motions it persists on long time scales. The model of McWilliams et al. provides the general framework for the dynamics of wave–current interactions. In addition to the deterministic part, the vortex force, which couples the total flow vorticity to the residual flow due to the waves, will have a part that is associated with the dissipative mechanism. At the same time the wave field will experience dissipation, and tracer advection is affected by the appearance of a dissipative term in the Stokes drift velocity. Consistency leads to other dynamic consequences: the boundary conditions are modified to take into account the diffusive process and proper mass/momentum balances at the surface of the ocean. In addition to formulating how a wave–current interaction model is modified by the presence of short-time events that induce dissipation, this study proposes a stochastic parameterization of dissipation. Its relation to other alternative parameterizations is given. Two focal reasons make stochastic parameterizations attractive: one can draw from extensive practical modeling experience in other fields, and it ties in a very natural way to a wealth of observational data via statistics.

1. Introduction

The aim of this paper is to show how dissipative effects on wave scales enter the evolution equations for the general wave–current interaction model developed by McWilliams et al. (2004, hereinafter MRL04). This model has a simpler predecessor, namely, the one developed by McWilliams and Restrepo (1999, hereinafter MR99). The latter model is, in fact, the shelf wave–current interaction model modified to account for basin scales. For expository reasons the MR99 model will be employed here to show details of how dissipation at wave scales enters the dynamics of waves and currents; implications to the shelf model are considered briefly. There are a variety of ways of pursuing the main goal of this paper, within the asymptotic machinery used in deriving MR99 and MRL04, but here the opportunity is taken to introduce a stochastic parameterization. A secondary goal of this paper is thus to illustrate how such a parameterization is applied.

Corresponding author address: Juan M. Restrepo, Departments of Mathematics and Physics, The University of Arizona, Tucson, AZ 85721.
E-mail: restrepo@physics.arizona.edu

Restrepo and Leaf (2002) have considered the effect of small-scale dissipation on the long time residual flow due to waves in a boundary layer, namely, on the Stokes drift velocity. We found that the dissipation in forced standing wave flows affects the Lagrangian fluid orbit in such a way as to create a net residual flow in addition to trapping cells that are reminiscent of the deterministic case. In the progressive wave case flow structure is steady in the mean, as it should be, but will have fluctuations in the fluid paths that can stall particle motion on intermediate time scales. The implications to transport can be significant if the tracers are capable of responding to the residual flow. In that study we used more empirical means, capable of dealing with the problem in question but not generally extendable to the cases considered here, that is, to the more complete interaction of the waves and currents.

It was Jansons and Lythe (1998) that set the author on the path exploited here (see also Vanden-Broeck 1999). They solve a Langevin differential equation that has a progressive wave drift term and an additive stochastic term. The conceptual leap that they make is to place more asymptotic prominence to the noise term than to the deterministic drift term. If there was a physical connection between their calculation and an actual

DOI: 10.1175/JPO3099.1

physical phenomenon, one would have to look at systems that are dominated by Brownian motion: time-periodic, low-Reynolds-number flows—microscopic phenomena. It is claimed here, however, that their framework can be adapted to the inertially dominated wave–current problem by enforcing certain compatibility conditions and scales that lead to MR99 and MRL04.

It will be helpful to mention a particular dissipative mechanism in order to fix ideas. Whitecapping will be that phenomenon. Whitecapping is a very common sea surface event; the episodes are short lived and random in their spatiotemporal distribution [for details and references see Hasselmann (1974) and Komen et al. (1984)]. A dynamic of whitecapping that has an obvious cause and effect is the dissipation it imparts on the waves and currents. The effective dissipation sometimes changes dramatically when a sudden change in wind strength and/or wind direction occurs. Whitecapping has no complete theory, and inclusion of its effects in ocean dynamics models is accomplished via parameterizations, some of which can be very sophisticated [WAMDI Group (1988); Alves and Banner (2003); Komen et al. (1994); see also Warner and McIntyre (1999) and their references]. Craig and Banner (1994) and Burchard (2001) focus on the connection between wave breaking and turbulence.

Two other ways to represent and parameterize the dissipative phenomena in question are those elaborated by Sullivan et al. (2004) and Melsom and Saetra (2004) (see also Melsom 1996). Sullivan et al. determine empirically a functional form for the dissipation term, such that the net dynamics of currents are well approximated by the additive action of dissipative and deterministic terms. The dissipative term is then constrained by stress–energetics balances. Whitecapping is parameterized as a collection of spatially impulsive random events. The approach of Melsom and Saetra (2004), on the other hand, is to posit that breaking events have a net effect on partitioning the energy into a conservative wave potential/kinetic energy and dissipation; the result of whitecapping is a sudden change in sea elevation/pressure or mass flux after a breaking event. The parameterization in Melsom and Saetra (2004) is then borrowed from standard turbulence production/dissipation. The fundamental conceptual similarity between these two approaches and the one to be presented here is that they all forego understanding of the breaking process itself (as compared to, say, some spectral and turbulence-based frameworks), opting instead for an empirical approach to modeling dissipation. The specific phenomena considered by Sullivan et al. (2004) and Melsom and Saetra (2004) are different, but, if discussion is limited to wave–current interactions, another fundamental similarity between these two strategies and the one presented here is the following: the model of Melsom and Saetra (2004) does not have a mechanism for momentum transfer from one wave frequency to another. Sullivan et al. (2004) subsumes all of these transfers, positing that in the end one can characterize the very long time limit and the large spatial scales as having a conservative current dynamic plus an effective dissipation. Thus, whatever wave energy cascades occur, these are characterized in the specific parameterization of the dissipative term. The stochastic parameterization in the context of wave–current interactions, using the asymptotic balances in MRL04, will turn out to convey elements of both aforementioned approaches: the expectation of momentum transfers between wave components will be akin to Melsom's conception of the breaking process, to lowest order: it is a result of the asymptotics, not the parameterization (the higher-order transfers within the MRL04 framework will be considered in a separate communication). The "universal" empirical function that captures breaking, as is done by Sullivan and collaborators, is found in the stochastic parameterization in the choice of noise model, ultimately determined by comparison to Lagrangian path data under breaking waves, and the dynamic equation for the evolution of the covariance, an equation posed in the Eulerian frame. In the stochastic parameterization the dissipation is constrained by suitable conservation laws, as is done by Sullivan and collaborators as well as Melsom's group, but it should be pointed out that this is the result of the dynamic balances within the asymptotic expansion in MRL04, not because of the use of some stochastic model.

Additive noise is nothing more than a reasonable modeling ansatz, as the noise may be better characterized as multiplicative; dissipation is additive in Sullivan et al. (2004) and Melsom and Saetra (2004). Assuming a multiplicative noise has a few technical issues that make it formally different to work with, the modeling procedure can be mostly inferred by working with the logarithm of the stochastic differential equation for the Lagrangian orbital path and relating the scaling to the additive case, which is featured in this study. In any event, whether noise is appropriately modeled as additive or multiplicative is a matter of experimental verification. That noise, modeled as a stochastic process, can be related to dynamic dissipation at macroscopic scales is one of the most common yet profound notions of theoretical physics of collective phenomena. It is suggested here that there should be a derivation of the dissipation due to breaking and whitecapping at macroscopic scales, those of the current scales, in some analogous way as in a theory for the kinematic viscosity in the momentum balance of fluids based on Brownian motions that occur at microscopic scales. However, it is not at all obvious what specific model of noise best captures the violent changes that might occur in the Lagrangian path of a fluid parcel subjected to whitecapping or changes related to other dissipative mechanisms, such as bottom drag. These would have to be determined from experiments or field data. The more familiar stochastic parameterizations of fluctuation/dissipation are the highly elaborate notions of turbulence or weak turbulence. Here, however, it is proposed that opting for a far less complex notion of dissipation can have some advantages: 1) stochastic modeling might offer a convenient and perhaps more natural way to connect experimental field data to modeling; 2) multiscale strategies and other constructive techniques might be more conveniently adopted; 3) there is a wealth of expertise in modeling phenomena in other fields that might be exploited; and, in the specific context of the MRL04 theory for wave–current interactions, 4) field data in the more natural Eulerian frame can be used to pin down the parameters that are relevant in the model with dissipation.

How dissipation at short time scales affects wave–current interactions is presented in section 2. The context will be the basin-scale model in MR99. How some aspects of MRL04, the more general shelf model, are modified by the presence of dissipation is considered in section 3. The basic strategy proposed here is to write down the equation for the Lagrangian orbital path as a function of three space dimensions and time in terms of the familiar deterministic velocity and an additive noise term. The three-dimensional vector noise term is spatiotemporally dependent and is described by a stochastic process. The multiscale/asymptotic technique is then applied to derive the Eulerian statement for nonconservative wave–current interactions. Section 4 consists of a simple computational example that will serve to illustrate the nature and significance of dissipation on the dynamics of simple waves and currents.

2. Dissipation on basin scales

MR99 derived a complete model for planetary-scale waves and currents under quasigeostrophic conditions, with attendant equations: a buoyancy, related to the pressure via hydrostatic assumptions, whose advection equation is coupled to waves and currents and a continuity equation that determines the vertical component of the velocity. Dissipation in the momentum equation is captured by an eddy viscosity, thus taking into account anisotropy in the surface Ekman layer. In this section the model is reintroduced in asymptotic form in order to derive in balanced form the effect of wave-scale dissipation.

Considered here is an oceanic region on the rotating earth containing a stratified, incompressible fluid, whose upper free surface is at $z = \eta(\mathbf{x}, t)$ and whose rigid lower boundary is at $z = -H(\mathbf{x})$. The vertical coordinate is aligned antiparallel to the local gravitational force and is denoted by z; $z = 0$ corresponds to a quiescent ocean surface and $\mathbf{z}$ will denote the unit upward-pointing vector. The position vector is denoted by $(\mathbf{x}, z)$, where the transverse or horizontal component is $\mathbf{x} = (x, y)$. Time is denoted by t.

In MR99 it was found that the lowest-order equations, time averaged over the fast wave period scales, representing the basin-scale interactions between currents and waves, are as follows: The dimensionless momentum equation, to leading order in the current velocity $\mathbf{v}^{(0)}$, is

$$\frac{\partial \mathbf{v}^{(0)}}{\partial T} - \mathbf{V} \times \mathcal{Z} + \nabla\Phi - b^{(0)}\mathbf{z} = \nu\nabla^2\mathbf{v}^{(0)}, \tag{1}$$

where the rectified velocity is $\mathbf{V} = \mathbf{v}^{(0)} + \mathbf{u}^S$, the combined local Coriolis and vorticity is $\mathcal{Z} = 2\Omega + \boldsymbol{\omega}^{(0)}$, and $\mathbf{u}^S$ is the Stokes drift velocity. The term on the right-hand side is a simple description of dissipation of exclusive significance at the long time scales T.

The generalized geopotential function is

$$\Phi = p^{(0)} + \frac{1}{2}\mathbf{V}^2. \tag{2}$$

Since $\mathbf{v}^{(0)}$ is incompressible, the elliptical problem that determines Φ is

$$\nabla^2\Phi = \nabla \cdot [\mathbf{V} \times \mathcal{Z} + b^{(0)}\mathbf{z} + \nu\nabla^2\mathbf{v}^{(0)}]. \tag{3}$$

On the free surface the pressure is equal to the atmospheric surface pressure. In deriving (1) the Eulerian velocity $\mathbf{q}$ had been decomposed into

$$\mathbf{q} = \varepsilon[(\mathbf{u}^w, w^w)(\mathbf{x}, z, t) + \varepsilon\,\mathbf{v}(\mathbf{x}, z, t, T)]. \tag{4}$$

The velocity $(\mathbf{u}^w, w^w)(\mathbf{x}, z, t)$, expressed in terms of its transverse and vertical components, is associated with the gravity wave field; the current is represented by $\mathbf{v}(\mathbf{x}, z, t, T)$. This description of the Eulerian velocity, as will be shown shortly, will be modified by the presence of stochasticity.

In MR99 the operator $\langle\,\rangle$ was an average over the faster time scale t, typified by the wave period $2\pi/\sigma_0$; dynamic quantities that still have time dependence after averaging will have dependence $T = \varepsilon^2 t$ (the averaging operator will be modified to handle noise later on). The small parameters $\varepsilon = k_0 a \ll 1$, with k_0 being the typical gravity wavenumber modulus and a being the typical amplitude of the waves. When the velocity is averaged over the fast time scales, the leading-order velocity is an approximation of the average current

$$\langle \mathbf{v} \rangle = \mathbf{v}^{(0)} + O(\varepsilon) = \langle \mathbf{q} \rangle / \varepsilon^2. \tag{5}$$

A compatible statement for the vorticity is

$$\langle \boldsymbol{\omega} \rangle = \boldsymbol{\omega}^{(0)} + O(\varepsilon). \tag{6}$$

There are also analogous expressions for the average buoyancy b and the tracer Θ, which in turn may be related to one another via an equation of state (see MR99). The relations among the nondimensional parameters are the following:

$$\Omega_0, \upsilon_0, N_0 = O(\varepsilon^2) \quad \text{and} \quad B_0, \tau_0, \mathcal{T}_0 = O(\varepsilon^4). \tag{7}$$

In order of appearance, these are the Coriolis, the long-time dissipation, the Brunt–Väisälä frequency, the buoyancy, the surface stress, and the surface tracer gradient.

The dimensionless boundary conditions are

$$w^{(0)} = \boldsymbol{\nabla} \cdot \mathbf{M} \quad \text{at} \quad z = 0, \tag{8}$$

where $w^{(0)}$ is the vertical component of the velocity, η^w is the sea elevation changes associated with the waves, and

$$\mathbf{M} \equiv \langle \check{\mathbf{m}} \rangle, \tag{9}$$

where

$$\check{\mathbf{m}} \equiv \mathbf{u}^w(\mathbf{x}, 0, t)\eta^w(\mathbf{x}, t).$$

In (8) the fact that the term $\langle D\eta^{(0)}/Dt \rangle$ is smaller by $O(\varepsilon^2)$ is used. Here $\eta^{(0)}$ is the leading-order sea elevation associated with the currents. On the other hand, if it were assumed that the horizontal variation of both the currents and wave statistics were on a slow scale $\mathbf{X} = \varepsilon^2 \mathbf{x}$, then the amplitude of $w^{(0)}$ would be smaller by ε^2 (for three-dimensional continuity balance), and the boundary condition (8) would be generalized by the addition of $\partial \eta^{(0)}/\partial T$ on the right-hand side. This addition would formally permit very long (i.e., shallow water) surface gravity waves in the current dynamics. The pressure equation is

$$p^{(0)} = \eta^{(0)} + p^a - P \quad \text{at} \quad z = 0, \tag{10}$$

where we have assumed that the slow atmospheric pressure variations p^a scale in a similar way to $p^{(0)}$, and the wave-added pressure adjustment term is

$$P \equiv \langle \check{p} \rangle, \tag{11}$$

where

$$\check{p} = \frac{\partial p^w}{\partial z}(\mathbf{x}, 0, t)\eta^w(\mathbf{x}, t) = \left(\frac{\partial \eta^w}{\partial t} \right)^2.$$

The slow-time surface stress condition is

$$\upsilon \left[\frac{\partial \mathbf{v}^{(0)}}{\partial z} + \mathbf{S} \right] = \tau \quad \text{at} \quad z = 0, \tag{12}$$

where

$$\mathbf{S} \equiv \langle \check{s} \rangle \tag{13}$$

is the wave-added correction, with

$$\check{s} = \frac{\partial^2 \mathbf{u}^w(\mathbf{x}, 0, t)}{\partial z^2} \eta^w(\mathbf{x}, t).$$

The leading-order tracer equation is

$$\frac{\partial \Theta^{(0)}}{\partial T} + \mathbf{V} \cdot \boldsymbol{\nabla} \Theta^{(0)} = \kappa \nabla^2 \Theta^{(0)}, \tag{14}$$

where the right-hand side term is a simple description of dissipation associated purely with the long time scales. The tracer surface boundary condition is

$$\kappa \frac{\partial \Theta^{(0)}}{\partial z} = \mathcal{T} \quad \text{at} \quad z = 0. \tag{15}$$

Further details on the derivation of the above equations are found in MR99. These equations will be modified by the presence of additive noise as follows.

The Lagrangian path, described by the position vector $\mathbf{Z}_t = (\mathbf{x}_t, z_t)$, of a fluid parcel with added stochasticity in three space dimensions and time will be assumed to be

$$\begin{aligned} d\mathbf{Z}_t = {} & \varepsilon(\mathbf{u}^w, w^w)(\mathbf{Z}_t, t)dt + \varepsilon^2 \mathbf{v}(\mathbf{Z}_t, T)dt \\ & + \mathsf{B}(\mathbf{Z}_t, t, T)d\mathbf{W}_t. \end{aligned} \tag{16}$$

The first two terms in the velocity correspond to the differential contribution of the deterministic part. These alone are consistent with the velocity field in MR99; see (4). The last term is the differential contribution of the velocity associated with noise, assumed attributed to the whitecapping events or other forms of dissipation at the short time scales, and modeled here as an additive vector-valued Wiener process $\mathbf{W}_t$; the 3×3 variance matrix B may have a slow and a fast temporal dependence as well as spatial dependence. The statistical description of the dissipation would be obtained from field data. The variance above is presumed to be dependent or parameterized by the transverse component of the position vector, which is taken to be the random process; the vertical component is thus random by the coupling of vertical and transverse components. The particle path, as given by (16), is consistent with the notion that at scales much shorter than the wave period the orbital path is Brownian; at scales comparable to the wave scale it is a combination of the orbit associated with the irrotational part of the velocity and stochasticity. At much larger time scales T, the velocity associated with currents enters the description of the path. The noise term, if properly chosen or derived, will conserve the Jacobian of the volumetric integrals of the velocity, albeit manifest temporal fluctuations, so that on average the incompressibility constraint is conserved. However, this term can also originate in some parameterized external force (or unresolved physics in an asymptotic setting of the equations of motion) that modifies the pressure in the flow, the gradient of which is a source of acceleration. Ultimately, a Langevin representation for the process of random fluctuations in the equations of motion, be it as additive or multiplicative, is a modeling choice with many appealing characteristics, one of which is simplicity and robustness [as compared with using a random velocity field, say—a far more complex notion; Olla and Paradisi (2004) and Klyatskin and Woyczynski (1995) show typical applications of the random velocity field concept to passive scalar evolution]. Here an ad hoc approach is taken, making the noise and variances in the transverse and the vertical direction two measurable degrees of freedom in the model. Uncertainty in the sea elevation phase can be thought of as accounting for the uncertainty in the pressure due to the wave dissipation and the uncertainty in the transverse velocity as a reflection of uncertainties in the transverse component of position.

In what follows the generality of the Langevin representation will be greatly simplified to suit modeling purposes. It will be assumed that the noise enters the dynamics via surface processes in the form of pressure fluctuations, which are in turn due to external forcing, for example, wind stresses, wave breaking, or some other type of dissipative process, such as losses ascribed to dissipation not related to whitecapping.

The wave sea elevation η^w is assumed to be composed of a linear superposition of individual components with different horizontal wavenumbers $\mathbf{k}_j$, each component given by

$$\eta_j^w = a_j \cos[\mathbf{k}_j \cdot \mathbf{x}_t - \sigma_j t - \sqrt{2\gamma_d}(W_j)_t + \theta_j]e^{-\gamma_d t}, \tag{17}$$

where γ_d is real, nonnegative, and $O(\varepsilon^2)$: it is the parameter associated with sea elevation dissipation due to propagation. Here $(W_j)_t$ is a zero-mean scalar Wiener process and θ_j is the sea elevation phase. These gravity waves arise primarily through the interaction of the wind with the ocean surface. Their dispersion relation is given by $\sigma_j = \sqrt{k_j}$.

Can fluctuations to the fluid orbital trajectory due to wave whitecapping be well captured by a Wiener process? It may be sensible to expect that breaking events produce orbital paths that are inherently extremely variable with paths that must be continuous (except for breaking that turns the fluid into a multiply connected entity) yet possibly with ill-defined differentials; whether it is Markovian in the strict sense is perhaps a matter of debate, but there is some consensus that the system would have extremely short memory at the time scales of interest here, that is, at current scales. Provided wave breaking leads to some dissipation, what is certainly reasonable is that some type of Wiener process can be a good vehicle to express its diffusive character. Brownian fluctuations may be a sensible characterization of the process, but perhaps the violence of the event would not be properly conveyed by a zero-mean stochastic model, especially if the wave is overturning very energetically. In any event, this or any other potential model could be verified experimentally. Figure 1a illustrates the noisy wave orbital path over about two wave periods. The transverse and vertical coordinates are arbitrary. The noise in this case is a Wiener process with zero mean and variance

$$\mathbf{B}(\mathbf{Z}_t, t, T) = D_0 \mathcal{W}(\mathbf{Z}_t, t, T; u^*), \tag{18}$$

where D_0 is a constant; $\mathcal{W} = 1$ here but, more generally, can be a process that is discrete in time, continuous in space, and possibly dependent on a wind speed threshold u^*. The noisy path is superimposed on the nonnoisy case. As shown in the figure, realizations of this process can generate fairly large fluctuations; however, the orbit has no trend. Figure 1b, on the other hand, shows the parcel path with a superimposed noise process of the form

$$\alpha_r(x - \ln x_t)x_t\,dt + \mathbf{B}\,dW_t^h, \tag{19}$$

where α_r is the mean reversion rate, x is the reversion mean, and $\mathbf{B}$ is as in (18). Figure 1c shows a mean-reverting process, as per (19), with the addition of the jump process $\kappa_r x_t dq_w$ (see Merton 1976). Here q_w is a discrete time Poisson process that, together with κ_r, depends on such things as the jump mean, variance, and jump frequency; it could also be made to depend on the wind speed u^*. This term can be made to handle very violent excursions of the particle path and, depending on the balance of this last term with the mean reverting ones, can be made to stay close or deviate significantly from the nonnoisy path. The parameters used in these figures are chosen simply to illustrate the qualitative differences among three simple models for the noise. Also, note that the deterministic wave orbital path formulas used here are not the actual water wave ones but the linearized ones. The point to emphasize here is that a suitable parameterization will connect field data to the Lagrangian or quasi-Lagrangian frame. However, one can also make contact with the Eulerian frame, and in what follows we derive the Eulerian statement for the momentum and continuity equations, using the additive Wiener process *ansatz*, for specificity.

Consistent with (17) the Lagrangian path, to lowest orders, is

$$d\mathbf{x}_t = \varepsilon \mathbf{u}^w dt + \sqrt{2B^h(\mathbf{X}, T)}\, d\mathbf{W}_t^h \quad \text{and}$$
$$d\mathbf{z}_t = \varepsilon \mathbf{w}^w dt. \tag{20}$$

The zero-mean components of the two-dimensional Wiener process $\mathbf{W}_t^h$ are assumed independent of W_t.

The lowest-order Lagrangian path $\mathbf{Z}_t^{(0)}$, for $t \geq 0$, is described by

$$\mathbf{x}_t^{(0)} = \sqrt{2B^h(\mathbf{X}, T)}\,\mathbf{W}_t^h \quad \text{and}$$
$$z_t^{(0)} = z. \tag{21}$$

Incorporating the lowest-order result, the Lagrangian path becomes

$$d\mathbf{x}_t^{(1)} = \sum_j a_j \sigma_j e^{kz_t} e^{-\gamma_d t}\left[\cos(\phi_j)\left(dt - \frac{D}{\sigma_j} dw_t\right) - \frac{\gamma_d}{\sigma_j}\left(1 + \frac{D^2}{2\gamma_d}\right)\sin(\phi_j)dt\right]\mathbf{k} \quad \text{and}$$
$$dz_t^{(1)} = \sum_j a_j \sigma_j e^{kz_t} e^{-\gamma_d t}\left[\sin(\phi_j)\left(dt - \frac{D}{\sigma} dw_t\right) - \frac{\gamma_d}{\sigma}\left(1 + \frac{D^2}{2\gamma_d}\right)\cos(\phi_j)dt\right], \tag{22}$$

where

$$\phi_j = (\mathbf{k}_j \cdot \mathbf{x} + Dw_t - \sigma_j t) \tag{23}$$

and

$$D = k\sqrt{2B^h(\mathbf{X}, T) + 2\gamma_d(\mathbf{X}, T)/k^2}. \tag{24}$$

Here w_t is the composite Wiener process. Strictly speaking, the asymptotic procedure makes the two Wiener processes lose independence from each other. From a practical standpoint this might be a moot point, as it might prove difficult to measure independently the parameters for the two stochastic processes. Nevertheless, these can be fixed, in principle, using independent conservation constraints. The spatial dependence of the variance has been taken to be at much larger scales than the typical wavelength of the gravity waves and thus approximately independent of the stochastic process $\mathbf{x}_t$. The dynamics of these waves, to leading order, are not influenced by the stratification; however, there is a wave-correlated component of the buoyancy and tracer fields, b^w and Θ^w, due to the stratification and an implied relationship between the buoyancy and tracers, as described in MR99. The $O(1)$ buoyancy has a wave solution

$$b_j^w = -\sum_j a_j e^{kz} \ddot{N}^2(z) e^{-\gamma_d t}\left[\cos(\phi_j)\left(dt - \frac{D}{\sigma_j} dw_t\right) - \frac{\gamma_d}{\sigma_j}\left(1 + \frac{D^2}{2\gamma_d}\right)\sin(\phi_j)dt\right], \tag{25}$$

with analogous relations for Θ^w. Here $\ddot{N}$ is the Brunt–Väisälä frequency. The pressure fluctuations are trivially related to the sea elevation and thus will have a stochastic component.

The vector and scalar field variables are decomposed into mean and fluctuating components. The averaging operator used in MR99 and MRL04 is now more general: the average of a quantity r, say, is given by

$$\langle \mathrm{En}[r(\cdot, T)]\rangle = \lim_{T_p \gg T^*} \frac{1}{T_p}\int_0^{T_p}\int_{-\infty}^{\infty} r(\cdot, \mathbf{x}, T, t')\Pi(\mathbf{x})\, d\mathbf{x}\, dt', \tag{26}$$

where $T_p \gg T^*$ is meant to convey that T_p should be sufficiently long relative to the time scale related to the variance of the noise and the length of the waves, that is, approximately $T_p \gg \lambda/kD_f$, where D_f is an estimate of the size of the variance; Π is the probability measure, which in the concrete examples to be shown later, is taken to be Gaussian. The new t average still

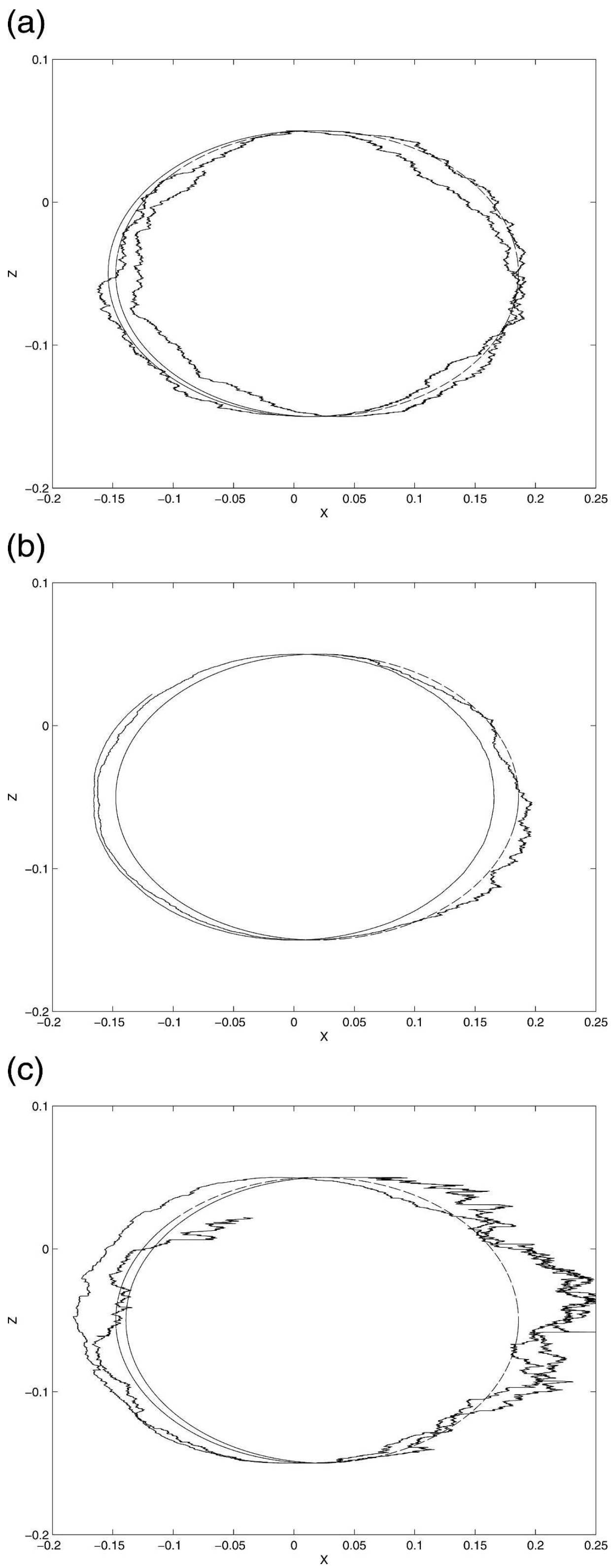

FIG. 1. Orbital path for linear waves plus noise modeled as (a) a Wiener process, (b) mean reverting plus Wiener, and (c) mean reverting with jumps and Wiener.

yields a quantity that varies at time scales typical of the longer wind and current variability; however, its interpretation is different.

Restating (22), the Lagrangian path to $O(1)$ is given by

$$d\mathbf{Z}_t^{(1)} = (\mathbf{u}^w, w^w)[\mathbf{Z}_t^{(0)}, t]dt, \tag{27}$$

which leads to

$$\mathbf{Z}_t^{(1)} = \int_0^t (\mathbf{u}^w, w^w)(\mathbf{Z}_s^{(0)}, s)\, ds. \tag{28}$$

At the next order

$$\frac{d\mathbf{Z}_t^{(2)}}{dt} = \int_0^t (\mathbf{u}^w, w^w)[\mathbf{Z}_s^{(0)}, s]\, ds \cdot \boldsymbol{\nabla}(\mathbf{u}^w, w^w)[\mathbf{Z}_t^{(0)}, t] + \mathbf{v}. \tag{29}$$

The first term is recognized, after averaging, as the Stokes drift velocity:

$$\mathbf{u}^s = \left\langle \mathrm{En}\left[\int_0^t \mathbf{u}^w(\mathbf{Z}_s^0, s)\, ds \cdot \boldsymbol{\nabla}\mathbf{u}^w(\mathbf{Z}_t^0, t)\right]\right\rangle, \tag{30}$$

with a dimensionalizing scale of $\varepsilon^2\sigma_0/k_0$.

Simple example: Basin-scale case

Consider the case of a monochromatic wave, as given by (17). It will be assumed in this example that the dynamics have a single transverse direction and depth dependence only. We will simplify (22) further by assuming that the $O(1)$ particle paths are given by

$$d\mathbf{x}_t^{(1)} = a\sigma e^{kz}e^{-\gamma_d t}\left[\cos(\phi)dt - \frac{\gamma_d}{\sigma}\left(1 + \frac{D^2}{2\gamma_d}\right)\sin(\phi)dt\right]\mathbf{k}$$

and

$$dz_t^{(1)} = a\sigma e^{kz}e^{-\gamma_d t}\left[\sin(\phi)dt - \frac{\gamma_d}{\sigma}\left(1 + \frac{D^2}{2\gamma_d}\right)\cos(\phi)dt\right]. \tag{31}$$

Explicit calculation of the transverse and vertical components of the Stokes drift velocity yields

$$\mathbf{u}^S(z, T) = a^2 k\sigma e^{2kz}[\mathbf{k}(1 - \gamma_d\Delta), \Delta - \gamma_d]\mathcal{D}. \tag{32}$$

Here $\Delta = (D^2 + 4\gamma_d)/4\sigma$ and

$$\mathcal{D} = \frac{e^{-2\gamma_0 T}}{1 + \Delta^2}.$$

It is noted that the exponential loss term was made to survive the time averaging, presumed appropriate because $\gamma_d t = \gamma_0 T$. When γ_d and D go to zero, we obtain the familiar deterministic result for the Stokes drift velocity with the vertical component identically zero. As shown by Jansons and Lythe (1998), it is also the case here that bidirectional wave fields can be constructed so as to cancel out the deterministic portion of the Stokes drift velocity and leave a nonzero diffusive part. A similar calculation yields

$$\mathbf{M} = \langle \mathrm{En}(\check{\mathbf{m}}) \rangle = \frac{1}{2} a^2 \sigma (1 - \gamma_d \Delta) \mathcal{D} \mathbf{k} \quad \text{and}$$

$$\mathbf{S} = k^2 \mathbf{M}, \tag{33}$$

and

$$P = \langle \mathrm{En}(\check{\mathbf{p}}) \rangle = \frac{1}{2} \sigma^2 a^2 e^{-2\gamma_0 T} \left(1 + \frac{\gamma_d^2}{\sigma^2}\right) \quad \text{and}$$

$$N = \langle \mathrm{En}(\check{n}) \rangle = \frac{1}{4} \sigma^2 a^2 e^{2kz} e^{-2\gamma_0 T} \left(1 + \frac{\gamma_d^2}{\sigma^2}\right), \tag{34}$$

with

$$\check{n} = \frac{1}{2}[(\mathbf{u}^w)^2 + (w^w)^2].$$

Quantities dependent on the Stokes drift velocity will also be affected by the presence of dissipation, namely, the tracer equation and the geopotential function Φ.

Contact between the observational data and the parameterization can be made in the Eulerian frame. For the two-component parameterization in the stress condition (12), the mass conservation (8) statements constrain the parameters. In this way the conservation statements are satisfied, in a spirit similar to Melsom (1996) and Sullivan et al. (2004). Both **S** and **M** in (33) can be written in terms of a contribution related to the deterministic wave contribution and another term. The other term has the two stochastic parameters. If the stochastic parameterization has only one component, then either the mass or stress conditions will suffice.

It is possible to endow the whitecapping parameterization with the spatially distributed discrete time impulsive character that Sullivan et al. (2004) use in their study of wave breaking effects on surface boundary layers: supposing, for simplicity, that $\lambda_d = 0$ ensembles of radar or photographic data over the swath of ocean of interest can be used to pin down the spatial aspect of the probability distribution of discrete-time jump processes that make up $\mathcal{W}$ in (18).

3. The shallow-water case

With the aim of making brief how the shelf case, its deterministic formulation appearing in MRL04 and Lane et al. (2007, hereinafter LRM07) is modified by the presence of dissipation we will make frequent reference to these two papers and modify the notation slightly to make the comparison easier. The main difference in the scaling, between the basin case and the shelf-scale case, is that in the latter there are three time scales: the fast wave scale t, the intermediate long-wave scale $\tau = \varepsilon^2 t$, and the current scale $T = \varepsilon^4 t$. Associated with these time scales is a short and long spatial scale, the latter being $\mathbf{X} = \varepsilon^2 \mathbf{x}$.

In MRL04 and LRM07, two averaging operators were defined, namely, the average over the fast scales and the average over intermediate or long-wave scales. The fast-time average is identical to (26); however, the symbol used in MRL04 for this average is the overbar. The average over intermediate scales was denoted by angle brackets. Both of these are modified, as in (26), by the need to ensemble average. Fluctuations at the long-wave time scale were denoted $(\,)^\dagger \equiv \overline{(\,)} - \langle\,\rangle$.

Adapting to the notation of LRM07 the particle path is described as

$$d\mathbf{Z}_t = \varepsilon \mathbf{U} dt + \mathsf{B}(\mathbf{Z}_t, t, \tau, T) d\mathbf{W}_t, \tag{35}$$

where

$$\mathbf{U} = (\mathbf{u}_0, w_0) + \varepsilon(\mathbf{q}^{\mathrm{lw}} + \mathbf{v}) + \varepsilon^2 \mathbf{u}^{\mathrm{wv}} + \varepsilon^3 (w^{\mathrm{lw}} + w^c). \tag{36}$$

The first term is associated with the linearized wave field. Here $\mathbf{q}^{\mathrm{lw}}$ is the long-wave velocity, and higher-order corrections to the linearized wave velocity carry the superscript wv. The current velocity is (v, w^c).

The jth spectral component of the leading-order velocity is

$$(\mathbf{u}_0)_j = \frac{a_j \mathbf{k}_j \cosh \mathcal{Z}_j}{\sigma_j \tanh\mu \cosh \mathcal{H}_j} \left[\cos(\phi_j) dt - \frac{\gamma_d}{\sigma_j}\left(1 - \frac{D^2}{2\gamma_d}\right) \sin(\phi_j) dt\right] \quad \text{and}$$

$$w_0 = \frac{a_j k_j \cosh \mathcal{Z}_j \tanh \mathcal{Z}_j}{\sigma_j \tanh\mu \cosh \mathcal{H}_j} \left[\sin(\phi_j) dt - \frac{\gamma_d}{\sigma_j}\left(1 - \frac{D^2}{2\gamma_d}\right) \cos(\phi_j) dt\right]. \tag{37}$$

The associated jth component of the sea elevation is

$$\eta_j^w = a_j e^{-\gamma_d T} \cos(\phi_j), \tag{38}$$

where ϕ_j is as given by (23), $\mathcal{H}_j = k_j \mu H$, and $\mathcal{Z}_j = k_j(z + \mu H)$; $\mu = k_0 H_0$ is a scaling parameter of order 1 in the shelf case, which arises naturally in the nondimensionalization (see MRL04), and $\gamma_d = O(\varepsilon^4)$ now owing to a change of time scales relevant to shelf dynamics. The equation for the complex amplitude for the waves is

$$\frac{dA_j}{d\tau} = \mathbf{C}_{g,j} \cdot \nabla_X A_j + \frac{1}{2} A_j \nabla_X \cdot \mathbf{C}_{g,j} + \frac{1}{2} iM_j|A_j|^2 A_j + \frac{ikA_j}{\sinh(2\mathcal{H}_j)}[\sigma_j Z + 2\int_{-\mu H}^{0} \cosh(2\mathcal{Z}_j)\mathcal{V}_j(z)\, dz], \tag{39}$$

where $C_{g,j}$ is the group velocity, $Z = \eta^{\mathrm{lw}} + \zeta$ is the long-time sea elevation, and $\mathcal{V}_j = \mathbf{k}_j \cdot (\mathbf{q}^{\mathrm{lw}} + \mathbf{v})$. The functions M_j and Z, which have a bearing on the phase but not on the amplitude of the complex A_j (described in MRL04), are modified by the presence of dissipation; however, their explicit calculation is omitted here. The wave dispersion relation is

$$\sigma_j^2 = \frac{k_j}{\tanh(\mu)} \tanh\mathcal{H}_j.$$

The evolution equations for the large spatiotemporal scale dynamics of the wavenumber and frequency will remain unchanged by the presence of dissipation.

a. Long-wave dynamics

The unforced conservative equations for the long-wave component of the flow are

$$\frac{\partial \mathbf{q}^{\mathrm{lw}}}{\partial \tau} + \nabla_X p^{\mathrm{lw}} = -\nabla_X \mathrm{En}(\breve{n})^{\dagger},$$

$$\frac{\partial p^{\mathrm{lw}}}{\partial z} = -\frac{\partial}{\partial z}\mathrm{En}(\breve{n})^{\dagger},$$

$$\nabla_X \cdot \mathbf{q}^{\mathrm{lw}} + \frac{\partial w^{\mathrm{lw}}}{\partial z} = 0,$$

$$w^{\mathrm{lw}}(-\mu H) + \mathbf{q}^{\mathrm{lw}}(-\mu H) \cdot \nabla_X(\mu H) = 0,$$

$$w^{\mathrm{lw}}(0) - \frac{\partial \eta^{\mathrm{lw}}}{\partial \tau} = \nabla_X \cdot \mathrm{En}(\breve{\mathbf{m}})^{\dagger},$$

and

$$p^{\mathrm{lw}}(0) - \frac{1}{\tanh\mu}\eta^{\mathrm{lw}} = -\mathrm{En}(\breve{p})^{\dagger}. \tag{40}$$

The fast-wave dynamics appear in these equations, imparting momentum and mass flux into the long-wave dynamics. Hence, even in the absence of forcing, the long waves can respond dynamically due to the waves (e.g., set up/set down). The quasi-static pressure and sea level are, respectively, $\hat{p}^{\mathrm{lw}} = -\{\mathrm{En}[\breve{n}(z)]\}^{\dagger}$ and $\hat{\eta}^{\mathrm{lw}} = \tanh(\mu)(-\{\mathrm{En}[\breve{n}(0)]\}^{\dagger} + \mathrm{En}[\breve{p})]^{\dagger})$ [cf. to MRL04's (6.3)].

Explicit calculation of the dissipative expressions is possible using a particularly simple form for the noise. To simplify, it is assumed that the wave field is monochromatic and that spatial dependence is in transverse and depth dimensions only. Assuming that the variance is of the form (24), the following are modified by the presence of surface dissipation:

$$\mathbf{M} = \left\{\frac{1}{2}\frac{a^2\sigma\hat{\mathbf{k}}}{\tanh(\mathcal{H})}\left[1 - 2\frac{\gamma_d}{\sigma}\Delta - \left(\frac{\gamma_d}{\sigma}\right)^2\right]\mathcal{D}\right\}^{\dagger}, \tag{41}$$

$$\mathbf{S} \equiv k^2\mathbf{M}, \tag{42}$$

$$P = \left\{\frac{1}{2}a^2\sigma^2 e^{-2\gamma_0 T}\left[1 + \left(\frac{\gamma_d}{\sigma}\right)^2\right]\right\}^{\dagger}, \quad \text{and} \tag{43}$$

$$N = \left\{\frac{1}{4\sinh^2(\mathcal{H})}a^2\sigma^2\cosh^2(\mathcal{Z}) \times \left[1 + \left(\frac{\gamma_d}{\sigma}\right)^2\right]e^{-2\gamma_0 T}[1 + \tanh^2(\mathcal{Z})]\right\}^{\dagger}. \tag{44}$$

b. Dissipation at current scales

Following the same strategy and assumptions as in section 3a, explicit forms of the averaged quantities can be computed. The quantities $\mathbf{M}$, $\mathbf{S}$, P, and N that appear above have the same form: however, the averages are now understood as being taken over the longer time scale T; that is, the average $\langle\,\rangle$ is used.

The Stokes drift velocity is

$$\mathbf{v}^{\mathrm{St}} = \left\langle \frac{a^2\sigma}{2\sinh^2(\mathcal{H})}\mathbf{k}\cosh(2\mathcal{Z})\left[1 - \frac{\gamma_d}{\sigma}\Delta + \frac{\gamma_d}{\sigma} \times \left(\frac{\gamma_d}{\sigma} + \Delta\right)\mathrm{sech}(2\mathcal{Z})\right]\mathcal{D}\right\rangle \tag{45}$$

and

$$w^{\mathrm{St}} = \left\langle \frac{a^2\sigma k}{2\sinh^2(\mathcal{H})}\sinh(2\mathcal{Z})\left(\frac{\gamma_d}{\sigma} + \Delta\right)\mathcal{D}\right\rangle.$$

When dissipative effects are not present it would be true that

$$w^{\mathrm{St}} = -\nabla_X \int_{-\mu H}^{z} \mathbf{v}^{\mathrm{St}} dz',$$

but this is not always the case, otherwise. The mass balance has to take into account a momentum flux due to the waves. The boundary condition at $z = 0$, as given by (9.12) in MRL04, is now

$$w^c(0) = \nabla_X \cdot \mathbf{T}^{\mathrm{St}}, \tag{46}$$

where $\mathbf{T}^{\mathrm{St}} = \langle \mathrm{En}(\breve{\mathbf{m}})\rangle$.

The static sea level and pressure fields, given by (9.8) in MRL04, are

$$\hat{\zeta} = -\frac{\tanh(\mu)}{\varepsilon}P_0 - N(0) + P \quad \text{and}$$

$$\hat{p}(z) = -\frac{1}{\varepsilon}P_0 - N. \tag{47}$$

The dynamic boundary condition, given by (9.9)–(9.11) in MRL04, is

$$\frac{1}{\tanh(\mu)}\zeta^c - p^c(0) = \hat{\zeta}\frac{\partial \hat{p}}{\partial z}(0) + \left\langle \eta^{\mathrm{lw}}\frac{\partial p^{\mathrm{lw}}}{\partial z}(0)\right\rangle + \frac{1}{\tanh(\mu)}\mathcal{P}_0, \tag{48}$$

where $\mathcal{P}_0$ is given in MRL04's (9.11) and LRM07's (3.7). It is convenient to redefine the vertical coordinate range to be $-H(\mathbf{x}) \le z \le \zeta + \hat{\zeta}$, rewriting the momentum equations with the quasi-static component of the pressure and sea elevation removed (see MRL04; LRM07); by doing so the calculation of $\mathcal{P}_0$ is not required. The Bernoulli head $\mathcal{K}$ [see (3.15) in LRM07] with the quasi-static components removed simplifies greatly as well. The modification owing to the presence of dissipation is that the Bernoulli head would appear multiplied by

$$e^{-2\gamma_0 T}\left(1 + \frac{\gamma_d^2}{\sigma^2}\right).$$

The momentum equations [(9.15) in MRL04] also have a vortex force term $\mathbf{J}$ and an adjustment to the quasi-static pressure K. These change owing to the new dissipative Stokes drift velocity. As a consequence of the asymptotics, there will also be an additive diffusion term akin to the current dissipation term proposed by Sullivan et al. (2004).

The tracer equation and buoyancy, as given by (10.7) and (11.12) in MRL04, include the Stokes drift velocity and thus will be affected by dissipation as well. The tracer evolution equation is also modified by changes in e^2 [see (10.8) and (10.9) in MRL04]:

$$\overline{e^2} = \frac{a^2 e^{-2\gamma_0 T}\sinh^2(\mathcal{Z})}{\sinh^2(\mathcal{H})}.$$

The gradient of the buoyancy modifies the long-time vorticity as well as the vertical momentum [see (11.12) and (11.13) in MRL04], and thus dissipation also modifies the momentum balance due to the stratification.

4. A numerical illustration

In MRL04 an example calculation was used to show that the interaction between waves and currents is significant (further comments related to this example appear in LRM07 as well). In that example we chose for

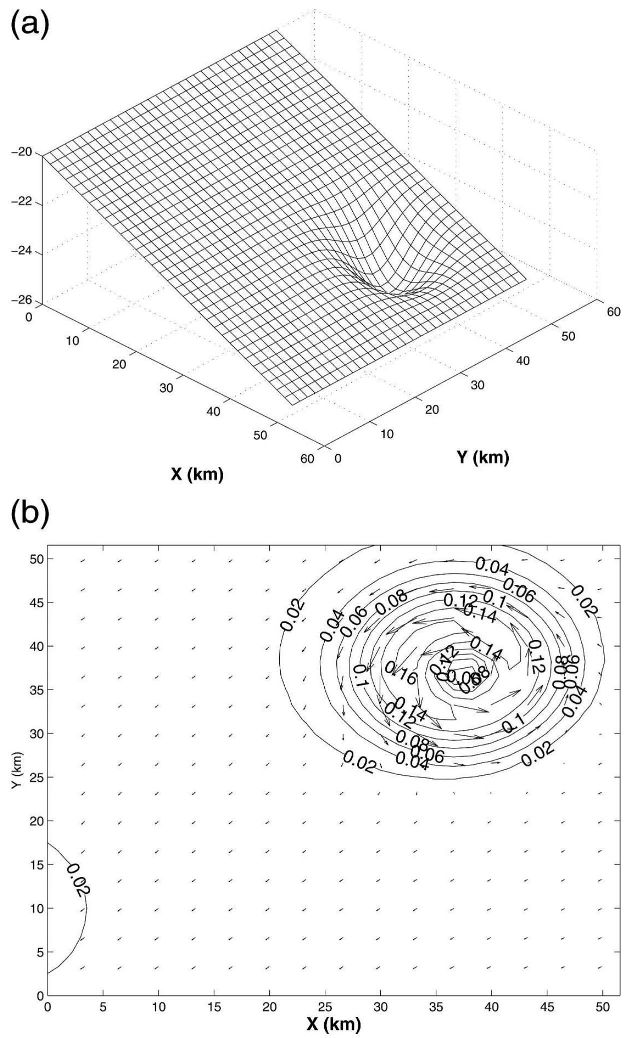

FIG. 2. (a) Bottom depth $H(\mathbf{X})$ (m). (b) Initial vortex velocity $\mathbf{v}(\mathbf{X}, 0)$ (m s^{-1}).

illustration to calculate the interaction of waves and currents on a broad shelf region with a gentle bottom slope up toward the west and a circular depression (Fig. 2a). The primary wave was specified to be incident from the deeper region to the east, propagating westward through the domain *en route* to a coastline farther west. The currents were dominated by a cyclonic vortex, initially centered over the bottom depression (Fig. 2b). We examined both wave and current solutions, but their mutual interaction was artificially constrained to simplify things: the wave field was in steady-state balance (on the τ scale) with the initial vortex, and the vortex evolution (on the T scale) was calculated with the wave field frozen in its initial state, rather than coevolving with the currents. Here the effect of dissipation on current scales is shown and compared to the case without dissipation, the MRL04 case. In the base-

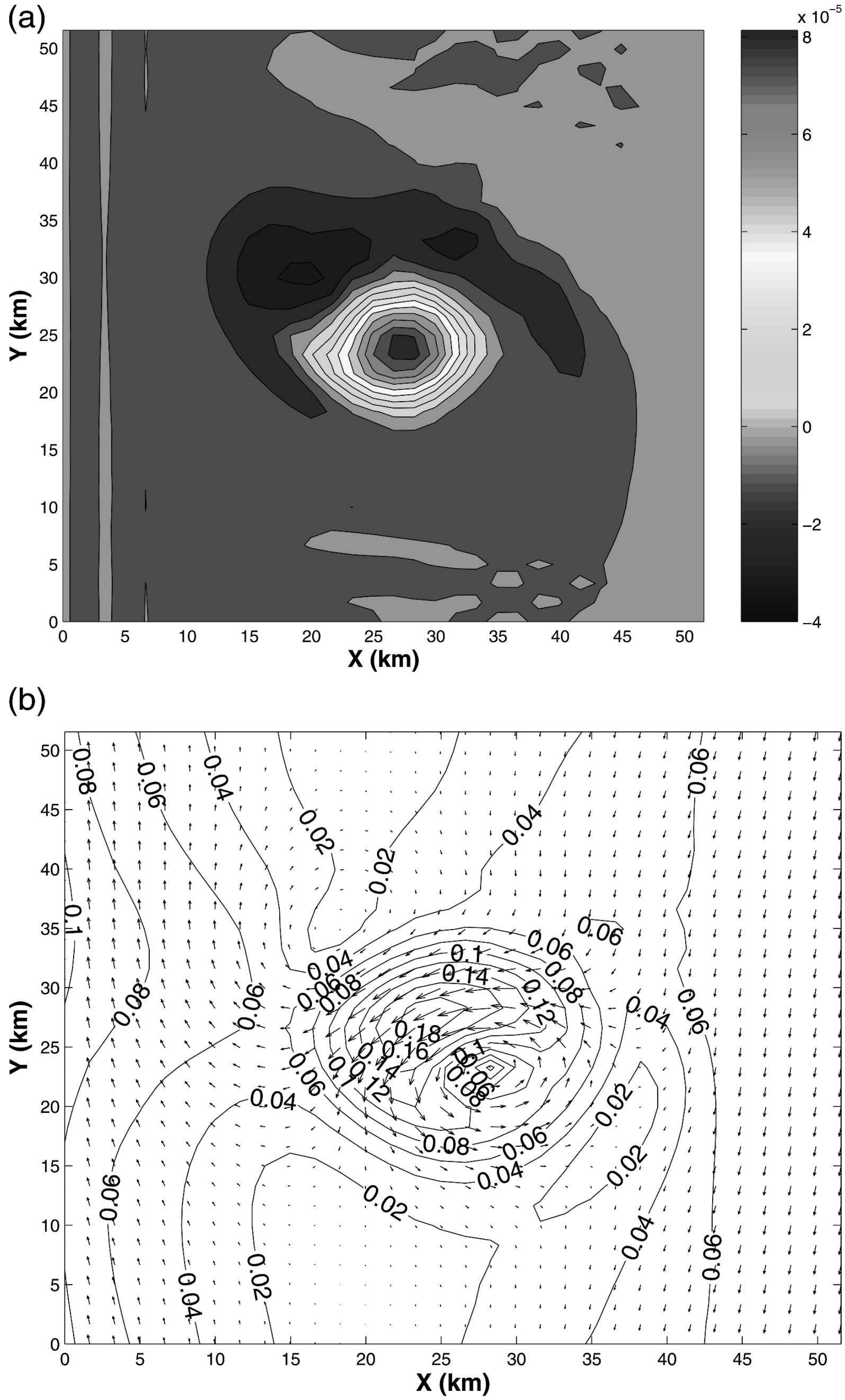

FIG. 3. (a) Vorticity $\mathcal{X}^c(\mathbf{X})$ (s^{-1}) and (b) velocity $\mathbf{v}(\mathbf{X})$ ($m\ s^{-1}$) (both as vector and contoured speed) for the currents in the baseline case at a time of $T = 4.0$ days.

line case for the wave evolution, the horizontal domain was a square with a span of $L = 56$ km. The resting depth decreases from 25 m in the east to 20 m in the west, and the superimposed depression was 2 m deep with a Gaussian decay on a spatial scale of 7 km and a center in the northeast quadrant. The incident wave was uniform along the eastern boundary. It had an amplitude of $a = 1.5$ m, slow phase of $\theta = 0$, wavelength of

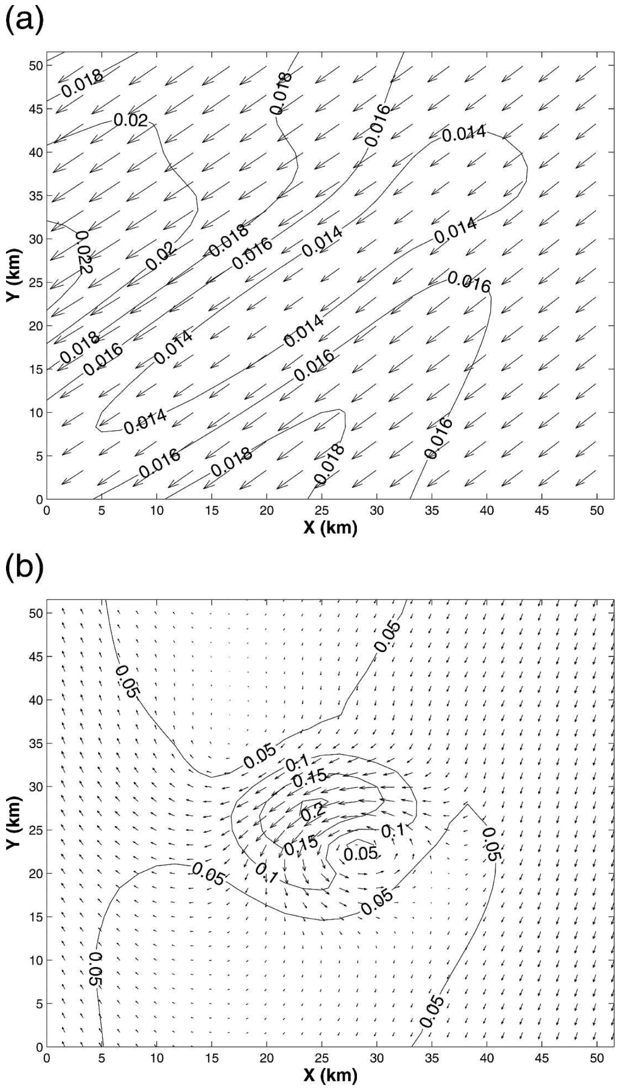

FIG. 4. (a) Stokes drift $\mathbf{v}^{St}(\mathbf{X})$ (m s^{-1}) and (b) the combined velocity $\mathbf{v} + \mathbf{v}^{St}(\mathbf{X})$ (m s^{-1}) (both as vectors and contoured speeds) in the baseline case at a time of $T = 4.0$ days.

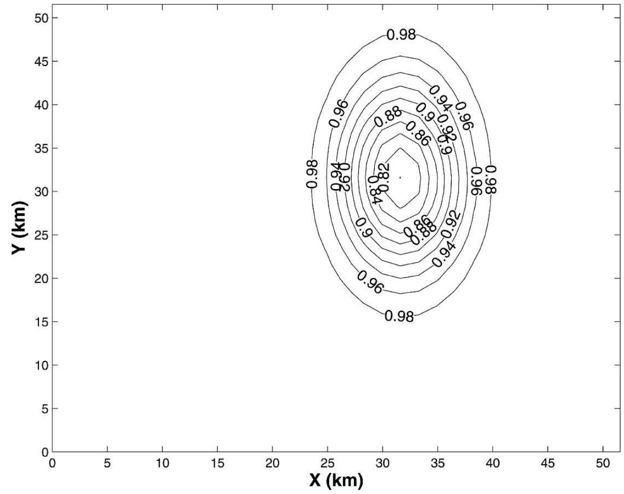

FIG. 5. Dissipation as a function of space.

$2\pi/k = 160$ m, and propagation direction to the southwest. The associated wave period was $2\pi/\sigma = 11.5$ s, phase speed was 13.6 m s^{-1}, and group velocity $|\boldsymbol{C}_g| = 10.5$ m s^{-1}. A cyclonic current vortex was centered over the bottom depression (Fig. 2b). It had a Gaussian shape for $\mathcal{X}^c(\mathbf{X})$ with a peak amplitude of 10^{-4} s^{-1}. The widths of both the depression and vortex were 7 km. The associated velocity field had a maximum speed of about 0.16 m s^{-1}. The initial cyclonic vortex (Fig. 2a) had a peak amplitude of 10^{-4} s^{-1} that was equal to f; hence the initial vortex Rossby number was one.

The calculations in MRL04 and those presented here made use of depth averaging and the suppression of any z dependence of all dynamical quantities. In the calculations the vertical component of the Stokes drift was suppressed and the drift velocity actually is used in its depth-averaged form. As shown in this study, if dissipative effects are important the vertical component of the Stokes drift is not simply given by an integral of the transverse component. In this two-dimensional calculation the vertical component of the Stokes drift is artificially suppressed, however.

Figure 3 reproduces the vorticity and velocity fields, after 4 days of evolution, when no dissipation is present. Figure 4 shows the Stokes drift and the combined velocity, with no dissipation. Figure 5 is a plot of the spatial dependence of the "dissipation function," which was used in the calculations and appears as multiplicative in the depth-averaged transverse components of the Stokes drift. The dissipation function is the expression appearing in brackets times $\mathcal{D}$ in the depth-averaged Stokes drift velocity, namely,

$$\frac{1}{4}\frac{a^2\sigma\mathbf{k}}{\sinh^2(\mathcal{H})}\sinh(2\mathcal{H}) \times \left[1 - \frac{\gamma d}{\sigma}\Delta + 2\mathcal{H}\frac{\gamma d}{\sigma}\left(\frac{\gamma d}{\sigma} + \Delta\right)\mathrm{csch}(\mathcal{H})\right]\mathcal{D}.$$

For simplicity, the wave dissipation γ_d has been set to zero and there is no time dependence in the variance and thus none in the dissipation. In this case the spatially dependent dissipation is $\mathcal{D}(\mathbf{X})$. This function was prescribed to produce a localized region of intense dissipation. This patch is stationary and present during the full 4-day simulation. The dissipation is maximally 28% higher in the epicenter of the localized region than in locations far away from it, where dissipation is made to die off.

The resulting vorticity and velocity, with dissipation present, are shown in Fig. 6. The depth-averaged transverse Stokes drift and the combined Stokes drift and current velocities appear in Fig. 7. The stress relation

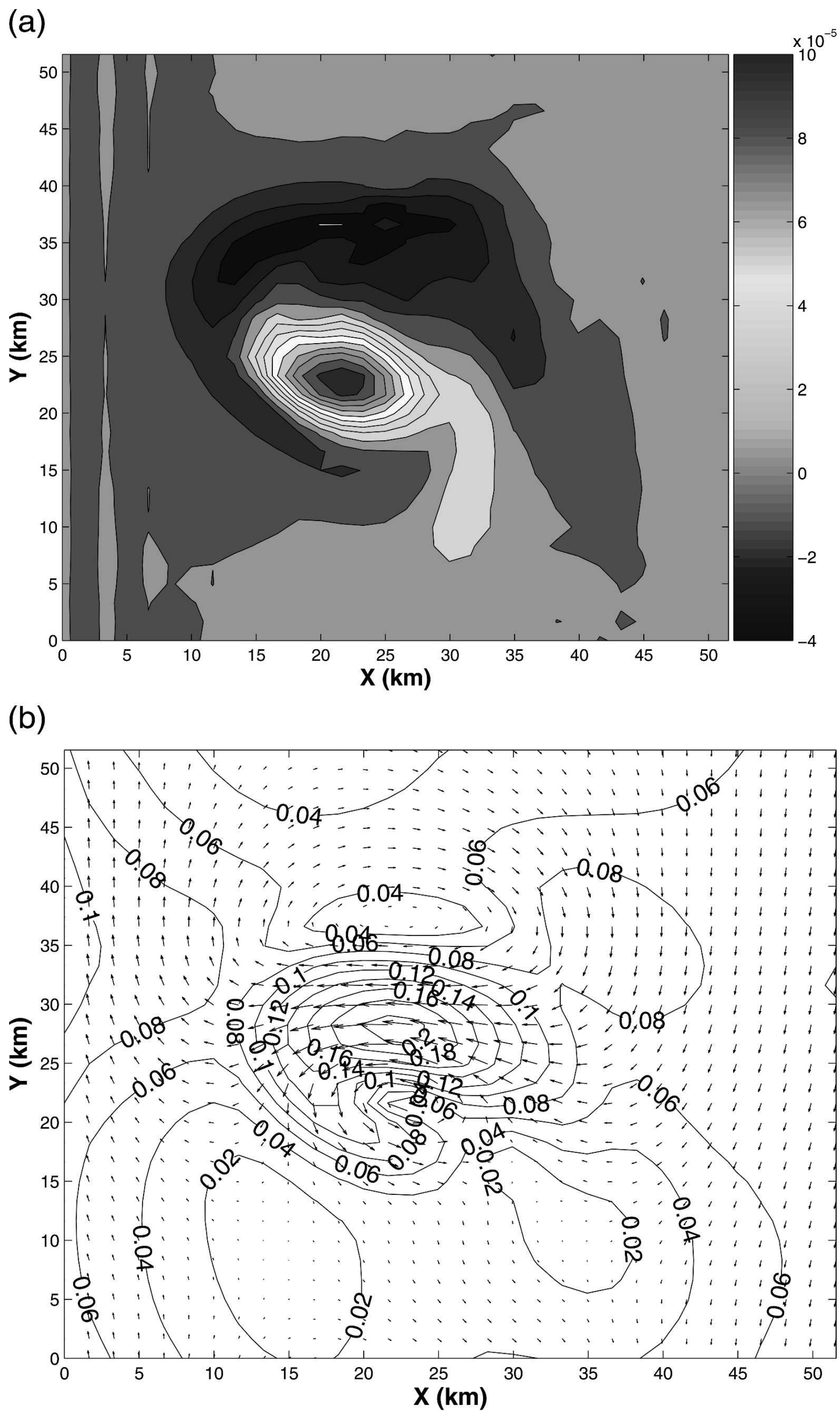

FIG. 6. (a) Vorticity $\mathcal{X}^c(\mathbf{X})$ (s^{-1}) and (b) velocity $\mathbf{v}(\mathbf{X})$ (m s^{-1}) (both as vector and contoured speed) for the currents in the baseline case at a time of $T = 4.0$ days, with dissipation. See Fig. 3 for comparison.

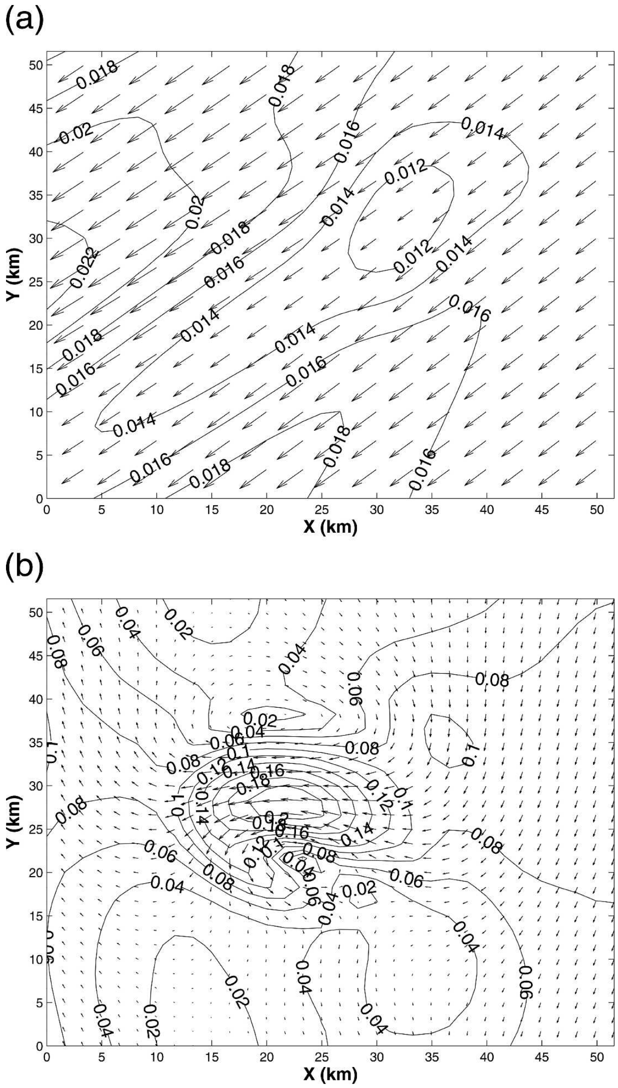

FIG. 7. As in Fig. 6 but for (a) Stokes drift $\mathbf{v}^{St}(\mathbf{X})$ (m s^{-1}) and (b) the combined velocity $\mathbf{v} + \mathbf{v}^{St}(\mathbf{X})$. See Fig. 4 for comparison.

(12) is used in the calculation to provide the currents with a body force with a strength equal to the difference between the nondissipative wave input and its dissipative counterpart.

5. Concluding remarks

This study showed that dissipative effects, at scales shorter than waves, survive large-scale averaging. The implications to the particular wave–current interaction model of McWilliams et al. (2004) were enumerated. An example of the type of dissipation considered is whitecapping. Stochastic parameterization was used to represent the dissipation. Standard parameterized wave attenuation was also included in the phenomenology, with the aim of showing how it might be implemented within the context of stochastic modeling. The approach used here is purely ad hoc and as such assumes that the dissipation parameters are obtained from data as there is no dynamic for the noise to lowest order. The lack of dynamics of both the waves and the dissipation is purely the result of the scaling appropriate to basin scales. In the context of MRL04, however, we expect to have a dynamic for the dissipation, but the specifics of this have yet to be worked out. In the specific wave–current interaction model considered here it is perhaps surprising that the noise does not enter as a small perturbation to the deterministic dynamics (the strong noise limit would seem more appropriate in low-Reynolds flows). However, the wave–current interaction model is fundamentally a time-scale ordering in which it is reasonable to assume that fluctuations induced by whitecapping occur at the very fastest of time scales and thus to lowest order.

It was shown here that dissipation modifies such quantities as the Stokes drift velocity, the pressure, and the vortex force and, thus, also modifies the radiation stresses. Dissipation also modifies how boundary conditions at the air–sea interface are applied.

The strategy employed was to assume that breaking leads to fluctuations in particle paths at time scales smaller than the wave time scale, as well as to uncertainties in the wave phase. The *e*-folding distance for the attenuation of the gravity waves due to other losses (e.g., surface contamination) was made large in accordance with what is assumed known about the propagation of these waves. The point of including such an effect was to show that it can be done within the context of the stochastic modeling in a manner consistent with the asymptotic balances of MR99 and LRM07.

How the Lagrangian paths were modified due to the presence of dissipation does not lead to a purely random velocity field but, rather, a velocity that has a stochastic component. The use of a Wiener process, as a model for the noise, was highlighted here for illustration. However, mention was made of other stochastic models that can incorporate such things as mean reversion, jump processes; furthermore, one can easily incorporate a random spatiotemporal distribution of point processes in order to mimic whitecapping due to gails in an extended domain, for example. The specific noise model would have to be determined with heretofore unavailable Lagrangian laboratory or field data. Ultimately, the model has parameters that have a spatiotemporal structure, which in turn are determined in the Eulerian frame by comparison to field data. For example, the spatial dependence of the variance would likely be an ensemble of ensemble averages of breaking occurrences and strengths over the ocean surface [as was done in Sullivan et al. (2004)].

There is nothing new with regard to representing noise and dynamics as a Langevin system. However, in doing so, we depart in a fundamental way in the manner in which wave breaking is commonly represented in ocean dynamics: a technique that has a long and distinguished history is spectral [Alves et al. (2003) is a recent article on this]. The Langevin model has been chosen with forethought: A great deal is known about the Langevin representation, and it is very flexible and robust. More importantly, there is a highly developed theory in stochastic differential equations and stochastic modeling that can be exploited in the context of making contact with data, be it in the Lagrangian or the Eulerian frame or a combination of both. The Langevin approach lent itself well to the multiscale/asymptotic strategy followed in MRL04 in deriving the conservative wave–current model. The Langevin representation along with stochastic parameterization is also convenient in lending itself directly to a variety of data assimilation schemes [for Lagrangian data assimilation, see Restrepo (2007)]. In due time the usual dialectic process will take place and the connection between the Langevin approach and the spectral approach to wave breaking will take place: the ideal place to make this connection is in a more general multichromatic stochastic wave–current interaction model [see Ding and Farmer (1994) and references contained therein on wave breaking statistics; see also Wu (1979)].

Although many of the quantities that contribute to the radiation stresses have been examined here, a derivation and the full impact of wave dissipation on these quantities has yet to be done. A sequel to this paper will develop further the stochastic parameterization and, with it, compute in detail the dynamic variables beyond the order which was done here. With this more complete model we will then investigate in detail how radiation stresses change in the presence of dissipation (a full derivation of the radiation stresses for the shelf setting due to wave–current interactions appears in LRM07). As presented in this study the dissipation itself has to be fully specified in space and in time. In the future a dynamic for the slow-time evolution of wave dissipation variance would be developed, leading to an evolutionary model for the interaction of waves, currents, and dissipative effects at all scales.

Acknowledgments. This research is supported by the National Science Foundation through Grant DMS0327642. The author thanks Jan Wehr, Grant Lythe, Rabinda Bhattacharya, and James McWilliams for their feedback and insights. This work was performed while the author was a visitor of the T7 group at Los Alamos National Laboratory.

REFERENCES

Alves, J. H. G. M., and M. L. Banner, 2003: Performance of a saturation-based dissipation-rate source term in modeling the fetch-limited evolution of wind waves. *J. Phys. Oceanogr.,* **33,** 1274–1298.

——, ——, and I. R. Young, 2003: Revisiting the Pierson–Moskowitz asymptotic limits for fully developed wind waves. *J. Phys. Oceanogr.,* **33,** 1301–1323.

Burchard, H., 2001: Simulating the wave-enhanced layer under breaking surface waves with two-equation turbulence models. *J. Phys. Oceanogr.,* **31,** 3133–3145.

Craig, P. D., and M. L. Banner, 1994: Modeling wave-enhanced turbulence in the ocean surface layer. *J. Phys. Oceanogr.,* **24,** 2546–2559.

Ding, L., and D. Farmer, 1994: Observations of breaking surface wave statistics. *J. Phys. Oceanogr.,* **24,** 1368–1387.

Hasselmann, K., 1974: On the spectral dissipation of ocean waves due to white capping. *Bound.-Layer Meteor.,* **6,** 107–127.

Jansons, K. M., and G. D. Lythe, 1998: Stochastic stokes drift. *Phys. Rev. Lett.,* **81,** 3136–3139.

Klyatskin, V. I., and W. A. Woyczynski, 1995: Fluctuations of passive scalar with nonzero mean concentration gradient in random velocity fields. *J. Theor. Exp. Phys.,* **81,** 770–773.

Komen, G. J., S. Hasselmann, and K. Hasselmann, 1984: On the existence of a fully developed wind-sea spectrum. *J. Phys. Oceanogr.,* **14,** 1271–1285.

——, L. Cavaleri, M. Donelan, K. Hasselmann, and S. Hasselmann, Eds., 1994: *Dynamics and Modelling of Ocean Waves.* Cambridge University Press, 532 pp.

Lane, E. M., J. M. Restrepo, and J. C. McWilliams, 2007: Wave–current interaction: A comparison of radiation-stress and vortex-force representations. *J. Phys. Oceanogr.,* **37,** 1122–1141.

McWilliams, J. C., and J. M. Restrepo, 1999: The wave-driven ocean circulation. *J. Phys. Oceanogr.,* **29,** 2523–2540.

——, ——, and E. M. Lane, 2004: An asymptotic theory for the interaction of waves and currents in coastal waters. *J. Fluid Mech.,* **511,** 135–178.

Melsom, A., 1996: Effects of wave breaking on the surface drift. *J. Geophys. Res.,* **101,** 12 071–12 078.

——, and O. Saetra, 2004: Effects of wave breaking on the near-surface profiles of velocity and turbulent kinetic energy. *J. Phys. Oceanogr.,* **34,** 490–504.

Merton, R. C., 1976: Option pricing when underlying stock returns are discontinuous. *J. Financ. Econ.,* **3,** 124–144.

Olla, P., and P. Paradisi, 2004: Relations between Lagrangian models and synthetic random velocity fields. *Phys. Rev.,* **E70,** 046 305, doi:10.1103/PhysRevE.70.046305.

Restrepo, J. M., 2007: A path integral method for data assimilation. *Physica D,* in press.

——, and G. K. Leaf, 2002: Wave-generated transport induced by ideal waves. *J. Phys. Oceanogr.,* **32,** 2334–2349.

Sullivan, P. P., J. C. McWilliams, and W. K. Melville, 2004: The oceanic boundary layer driven by wave breaking with stochastic variability. I: Direct numerical simulation of neutrally-stratified shear flow. *J. Fluid Mech.,* **507,** 143–174.

Vanden-Broeck, C., 1999: Stokes' drift: An exact result. *Europhys. Lett.,* **46,** 1–5.

WAMDI Group, 1988: The WAM Model—A third generation ocean wave prediction model. *J. Phys. Oceanogr.,* **18,** 1775–1810.

Warner, C. D., and M. E. McIntyre, 1999: Toward an ultra-simple spectral gravity wave parameterization. *Earth Planets Space,* **51,** 475–484.

Wu, J., 1979: Distribution and steepness of ripples on carrier waves. *J. Phys. Oceanogr.,* **9,** 1014–1021.